

N O T I C E

THIS DOCUMENT HAS BEEN REPRODUCED FROM
MICROFICHE. ALTHOUGH IT IS RECOGNIZED THAT
CERTAIN PORTIONS ARE ILLEGIBLE, IT IS BEING RELEASED
IN THE INTEREST OF MAKING AVAILABLE AS MUCH
INFORMATION AS POSSIBLE

NASA Technical Memorandum 81403

(NASA-TM-81403) ANALYSIS OF WEAR-DEBRIS
FROM FULL-SCALE BEARING FATIGUE TESTS USING
THE FERROGRAPH (NASA) 22 p HC A02/MF A01

CSCL 13H

N80-16341

Unclas
46948

G3/37

**ANALYSIS OF WEAR DEBRIS FROM
FULL-SCALE BEARING FATIGUE
TESTS USING THE FERROGRAPH**

William R. Jones, Jr. and Stuart H. Loewenthal
Lewis Research Center
Cleveland, Ohio



Prepared for the
Annual Meeting of the American Society of Lubrication Engineers
Anaheim, California, May 5-8, 1980

ANALYSIS OF WEAR DEBRIS FROM FULL-SCALE BEARING FATIGUE

TESTS USING THE FERROGRAPH

by William R. Jones, Jr. and Stuart H. Loewenthal

National Aeronautics and Space Administration
Lewis Research Center
Cleveland, Ohio 44135

ABSTRACT

The Ferrograph was used to determine the types and quantities of wear particles generated during full-scale bearing fatigue tests. Deep-groove ball bearings made from AISI 52100 steel were used. A MIL-L-23699 tetraester lubricant was used in a recirculating lubrication system containing a 49- μ m absolute filter. Test conditions included a maximum Hertz stress of 2.4 GPa, a shaft speed of 15 000 rpm, and a lubricant supply temperature of 74° C (165° F). Four fatigue failures were detected by accelerometers in this test set. In general, the Ferrograph was more sensitive (up to 23 hr) in detecting spall initiation than either accelerometers or the normal spectrographic oil analysis (SOAP). Four particle types were observed: normal rubbing wear particles, spheres, nonferrous particles, and severe wear (spall) fragments.

INTRODUCTION

The goals of oil analysis are to diagnose the current condition of operating machines and to be able to predict any future problems. A variety of different techniques (ref. 1) are being employed to effect these goals. These include spectrographic oil analysis (SOAP), magnetic chip detectors, vibration sensors, and particle counters. Although each of these techniques has certain advantages, most of the techniques suffer from not being able to distinguish among the various wear modes that can occur.

The Ferrograph has been developed to magnetically precipitate wear debris from used lubricants onto a glass slide to yield a Ferrogram (refs. 2 to 4). The precipitated particles range from approximately 0.02 to a few micrometers and are arranged according to size on the slide. Individual particles may be observed with a unique bichromatic microscope, the Ferroscope, or with a conventional scanning electron microscope.

A number of investigators (refs. 5 to 10) have identified the characteristic wear particles associated with the various wear mechanisms. In particular, three particle types have been observed during rolling-element fatigue: spheres, spall particles, and laminar particles (ref. 10). In fact, the occurrence of spherical particles in oil samples has been suggested to be a precursor of bearing fatigue in some cases (refs. 9 to 11). Recently, the Ferrograph was used to characterize the wear debris generated in accelerated rolling-element fatigue tests (ref. 12). Although spheres and microspall particles were observed in that study, their detection as a function of time was of limited use

in predicting fatigue failures. It was felt that this result may have been related to the accelerated nature of those tests (high maximum Hertz stress levels of 5.5×10^9 Pa were employed).

The objectives of this investigation were to (1) determine the types and quantities of wear particles generated in full-scale bearing fatigue tests by Ferrographic analysis and (2) determine the relative sensitivity of the Ferrograph compared to an accelerometer system in detecting spall initiation. Tests were conducted on a multiple bearing fatigue test machine with 65-millimeter bore diameter, deep-groove ball bearings lubricated with MIL-L-23699 qualified tetraester oil. Test conditions consisted of a shaft speed of 15 000 rpm, a radial load of 4580 newtons (1030 lb) and an oil inlet temperature of 74°C (165°F).

APPARATUS

Bearing Fatigue Tester

A cross section of the bearing fatigue tester used in this investigation is shown in figure 1. This tester is described in detail in reference 13. Two identical bearing fatigue testers, each containing four test bearings, were operated concurrently. Each bearing tester is driven by a quill shaft system connected to the 37.3 kilowatt (50 hp) variable speed drive system (not shown in the illustration). The bearings are loaded only in a radial direction by a hydraulic cylinder. The radial load is transmitted equally to the two center bearings through a wiffletree and is transmitted to the two outboard bearings as shown. Thermocouples were attached to the outer race of each test bearing.

The lubrication supply system, shown schematically in figure 2, delivers a total of 1090 kilograms per hour (2400 lb/hr) of oil through the test filter to the eight test bearings. The flow is equally divided among the test bearings by a calibrated orifice at an oil supply pressure of 0.28 megapascals (40 psi). Each test bearing was lubricated by its own calibrated oil jet. A total of 3×10^{-2} cubic meter (8 gallons) of lubricant was contained in the lubrication system. About 6×10^{-3} cubic meter (1.6 gallons) was removed from the system daily and replenished with fresh lubricant.

The oil drains from the test bearings by gravity into a collector pan and is returned to the oil supply tank by a scavenge pump. On this return line is an oil-water heat exchanger that regulates the oil inlet temperature to the bearings at the required 74°C (165°F). An automatic oil sampler is located in this return line. The sampler uses a plunger containing about a 4×10^{-6} cubic meter (4 ml) cavity which sweeps across the oil line cross-section when actuated. The sampler was cycled for about 50 seconds to fill a 1×10^{-4} cubic meter (100 ml) bottle.

The test stand instrumentation included an accelerometer system which detected bearing failures as well as protective circuits which shut down the drive system if any of the test parameters deviated from the programmed conditions. Parameters monitored and recorded during the test included bearing inner race speed, oil flow to each tester, test bearing outer race temperature, lubricant supply and scavenge temperature, and bearing vibration level.

Vertical and horizontal accelerometers were mounted on the case of each test head. The presence of a spall on either bearing race would cause a significant increase in the g-level. The nominal output of the accelerometers of 0.1 to 0.2 V would increase to more than 1.0 V causing rig shutdown. A signature analysis of the bearing vibrations was not involved.

The filter used in this study was a 30-micrometer nominal (MIL-F-5504) full-flow filter. It had a mean particle removal rating of 40 micrometers and an absolute rating of 49 micrometers (MIL-F-27656). It was of the porous depth-media type, composed of resin impregnated organic/inorganic fibers.

The lubricant used was a prefiltered neopentyl-polyolester (tetraester) meeting the MIL-L-23699 specification. Table I lists some of its typical properties.

Bearings

The bearings used in this study were ABEC-3 grade, deep-groove ball bearings with a 65-millimeter bore diameter containing 18 balls, each having a 7.94-millimeter diameter. The races and balls were manufactured from a single heat of carbon vacuum-degassed (CVD) AISI E-52100 steel. The nominal hardness of the races was Rockwell C62 \pm 1.0. The retainer was a machined two piece inner-land riding cage made from iron silicon bronze. The raceways were ground to a nominal surface finish of 0.1 micrometer rms and the balls to 0.05 micrometer rms. An overall view of a test bearing is shown in figure 3.

WEAR DEBRIS ANALYSIS

Ferrograph

The Ferrograph (refs. 2 to 4) was used to magnetically precipitate wear particles from the used oil onto a specially prepared glass slide. The oil sample was heated to 70° C for a minimum of 10 minutes and then shaken vigorously. A mixture of 3×10^{-6} cubic meter (3 ml) of used oil and 1×10^{-6} cubic meter (1 ml) of solvent is then prepared. This mixture is slowly pumped over the slide as shown in figure 4. A solvent wash and fixing cycle follows which removes residual oil and permanently attaches the particles to the slide. The resulting slide with its associated particles is called a Ferrogram.

The amount of wear debris on a Ferrogram was determined by measuring the optical density (percent are covered) of the deposit at seven positions along the slide - entry (55-56), 54, 50, 40, 30, 20, and 10 millimeters from the end of the slide. A composite Ferrogram density was determined for each slide by averaging the seven readings.

Energy Dispersive X-ray Analysis

The elemental composition of the different types of wear debris was determined using energy dispersive X-ray analysis. In order to prevent charging in

the scanning electron microscope, the Ferrogram slides were coated with either a thin layer (2×10^{-8} m, 200 Å) of carbon or gold.

RESULTS AND DISCUSSION

The lubricant samples analyzed in this study were selected from the larger fatigue test program reported in reference 13. Samples were taken at approximately 6- and 12-hour intervals from the lubrication line, downstream of the bearings, between the scavenge pump and supply tank as shown in figure 2. These samples were from a test set which resulted in four fatigue failures at 443, 526, 1013, and 1096 hours, respectively. The exact time of failure initiation is uncertain. However, the length of the spall is somewhat indicative of the time interval between spall initiation and detection due to high vibration levels. Table II contains the sizes of the spalls and the weight loss for each bearing.

The fatigue spall which was detected at 526 hours is illustrated in figure 5(a). A scanning electron micrograph of this spall is shown in figure 5(b) at low magnification and in figure 5(c) at higher magnification. This failure, which is typical of the failures in this test series, appears to be of the classical subsurface originated type.

Types of Wear Debris

Essentially four types of wear debris were observed during this study. These types were normal rubbing wear particles, spherical particles, nonferrous particles, and severe fragments. Fatigue microspall particles and laminar particles sometimes reported during fatigue tests (ref. 10) were not observed in this study.

Almost all of the oil samples of this study were exceptionally clean (i.e., they contained very few particles). Typically, Ferrogram composite density measurements were less than 1 percent (for a 3×10^{-6} m³ (3 ml) sample).

Normal rubbing wear particles. - Normal rubbing wear particles (ref. 10) are observed in almost all oil samples from lubrication systems. This study was no exception as most samples yielded at least a few such particles. Typically, these particles are small asymmetrical metallic flakes (<15 µm in major dimension and <1 µm thick). They are produced anytime that sliding wear takes place. Electron micrographs of some normal rubbing wear particles appear in figures 6(a) and (b). An X-ray energy map for iron appears in figure 6(c) and indicates that most of the particles are predominately iron.

This particle type is not related to the fatigue process. Moderate amounts of rubbing wear particles were observed in the samples taken at test startup and at 2 and 5 hours. This is related to the wear-in process and possible startup contamination. Throughout the rest of the test, few rubbing wear particles were observed. One possible source for these particles is the gear-type scavenge pump (fig. 2) located upstream of the automatic sampler.

Spherical particles. - Microspheres (1- to 10- μ m diam) were observed in many samples. An 8-micrometer sphere is shown in figure 6(a). Although most of the spheres appeared metallic when observed in the bichromatic microscope, an X-ray energy analysis indicated that there were two types present. These types are illustrated in figure 7 where two different 4-micrometer-diameter spheres are shown. An iron X-ray energy map for the sphere of figure 7(a) appears in figure 7(b). This is the normal iron map one would obtain from a solid iron or steel microscope. However, the 4-micrometer-diameter sphere of figure 7(c) indicates a much lower concentration of iron. This type of sphere may contain a large amount of organic material (ref. 14) or may be a compound of iron (an inclusion) (ref. 15) or perhaps even be hollow (ref. 16). Although an analysis of all the spheres observed during this study was not possible, measurements on a number of Ferrograms indicated about half of them contained a high concentration of iron and the remaining half a much lower concentration.

Nonferrous particles. - Several samples contained metallic nonferrous particles. In particular, two of the oil samples (429 and 435 hr) prior to the 443-hour failure contained this particle type. An optical micrograph of one such particle appears in figure 8(a) and its accompanying electron micrograph is shown in figure 8(b). These particles appear bronze-like in reflected white light and an X-ray energy analysis confirms this. X-ray energy maps for copper and zinc appear in figures 8(c) and (d), respectively. An analysis of the iron-silicon bronze bearing retainer closely resembles that of these particles. Therefore, it seems likely that the retainer is the source of these particles.

Severe wear particles. - Severe wear particles refer to large metallic ($>20 \mu\text{m}$ in major dimension) wear fragments which are the result of some catastrophic wear mode. Most of the severe particles observed in this study appeared to be spall fragments, since they were usually observed just prior to or after a fatigue failure. However, considering the rather large spalls that occurred, it is surprising that so few were observed. Either the spalling occurred very rapidly or the filtration system was efficient enough to greatly limit their concentration. Another possibility is that the large particles may have been comminuted in passing through the scavenge pump. After the test rig was shut down following each failure, the test head was completely cleaned and flushed out. Therefore, one would not expect to observe a large number of these particles after failure.

Correlation of Ferrogram Results with Fatigue Failure

As previously mentioned, composite Ferrogram densities were determined for each sample. This parameter yields the average particle density for each sample. A second parameter, the wear severity index, has been advocated by Bowen and Westcott (ref. 10). This parameter is calculated from optical density measurements made at the entry position of the Ferrogram (A_L) and at the 50-millimeter position (A_S). These are the areas covered by the large and small particles. Their sum ($A_L + A_S$) yields the general level of wear, while their difference ($A_L - A_S$) gives an indication of abnormality. These two quantities multiplied together ($(A_L + A_S)(A_L - A_S)$), yield the wear severity index, $A_L^2 - A_S^2$, usually abbreviated as I_S . In this study, increases in I_S are generally related to increases in the number of spall fragments.

The progression of the fatigue process has been studied by other investigators (refs. 6 to 11). In those studies, a precursor to fatigue failure has been the appearance of metallic microspheres in the lubricant. In addition, microspall particles and laminar particles sometimes appear in the oil prior to failure.

In a previous paper by the author (ref. 12) microspheres and microspall particles were observed in some accelerated rolling-element fatigue tests but not in all tests. In these tests of reference 12, optical density measurements were of little use in following fatigue progression because of contaminating "friction polymer" deposits.

In the present study, three parameters were followed as a function of test duration. These were the composite Ferrogram density, the wear severity index, and the number of microspheres. These parameters appear in figure 9 as a function of test time.

As can be seen, all three parameters yielded relatively high values during the first few hours of the fatigue test. The appearance of a large amount of debris during run-in is not unusual. However, the high initial sphere count in the 3-hour sample is not understood. As the test progressed, average background levels of about 2 for the number of spheres, less than 8 for the wear severity index, and less than 1 for the composite density were observed.

First fatigue failure (443 hr). - Discounting the run-in period, there were only a few samples that yielded values greater than the background levels for the wear severity index I_s and composite density during the first 400 hours (fig. 9). An examination of the particles present in these samples indicated a general increase in the amount of debris but no particles were observed which would be related to fatigue. However, 20 hours before the first fatigue failure was detected by the accelerometers, a few spall fragments were observed (423 hr sample). In the next sample (429 hr) there was a dramatic increase in the number of spheres (2 to 49), more spall fragments were noted, and a few bronze-like particles were observed. Similar results were obtained with the next sample (435 hr) but the sphere count had decreased to 10. Normal background levels were then observed in the 441-hour sample. Two hours later (443 hr) the accelerometer detected the first spall.

Second failure (526 hr). - Twenty-three hours before this failure was detected (503 hr) a sphere count of 12 was noted and spall particles were observed. The next sample (515 hr) yielded a similar sphere count, more spall fragments, and a large increase in I_s . Eleven hours later (526 hr) this failure was detected by the accelerometers. After the failed bearing was replaced and the test was restarted, spall particles were observed in the next three samples (530, 542, and 554 hr) and a higher than normal sphere count (14) was observed in the 530-hour sample.

Third (1013 hr) and fourth failure (1096 hr). - Fewer samples were analyzed after the second failure because of time limitations. Samples returned to background levels until the 897 hour sample, which yielded a few bronze-like particles and an accompanying increase in I_s . Two samples later, I_s increased again but no abnormal particles were observed. The 1005-hour sample appeared

normal but had a sphere count of 13. Eight hours later the fatigue failure was detected (accelerometer). The sample taken at shutdown was normal except for a few spall fragments. However, the next sample (1021 hr) yielded more spall particles, a sphere count of 16, and a very large increase in I_s . A few spall particles were observed at 1032, 1044, and 1073 hours, but other parameters were normal. The final failure was detected (accelerometer) at 1096 hours. The sample taken at that time yielded a sphere count of 12, a few spall particles, and a high I_s value.

In analyzing these results, it appears that spall initiation occurred more than 20 hours before accelerometer detection for the first failure, 23 hours before the second, and 8 hours before the third. It is not clear when spall initiation occurred in the fourth failure. The large increase in parameters in the 1021-hour sample is most likely an aftermath of the 1013-hour failure. The final spall was probably initiated sometime after the 1085-hour sample, propagated rapidly, and was detected by the accelerometers before the next routine sample was to be taken.

It should be noted that the accelerometer sensitivity was not optimized in this study. It is likely that a more sensitive accelerometer setting would have allowed for earlier failure detection. However, this would also increase the chance of spurious signals stopping the test before a failure occurred.

Spectrographic Oil Analysis

One other parameter was studied for possible failure correlation. This parameter was the change in concentration of iron in the oil samples measured by ordinary spectrographic analysis (SOAP). Measurements were only made on selected oil samples from test startup to 566 hours, thus encompassing the first two fatigue failures. The iron concentration in parts per million appears as a function of test time in figure 10. Rather low values were observed (0 to 3 ppm), and there was no correlation with the two failures.

CONCLUDING REMARKS

In general, the Ferrograph proved to be more sensitive in detecting spall initiation than the accelerometers or normal spectrographic oil analysis. Particles normally associated with fatigue were observed in the lubricant from 8 to 23 hours before accelerometer detection for three of the failures. For the fourth failure, these particles were observed only in the lubricant sample taken at test shutdown.

SUMMARY OF RESULTS

The Ferrograph was used to characterize wear debris from full-scale bearing fatigue tests. Four fatigue failures were detected by accelerometers at 443, 526, 1013, and 1096 hours. The results are summarized as follows:

1. In three of the four failures, there were increases in the number of spheres, the wear severity index, and the composite Ferrogram density prior to failure detection by accelerometers.

2. There was no correlation between the fatigue failures and iron concentrations in the lubricant as measured by ordinary emission spectrometer techniques (SOAP).

3. In general, lubricant samples contained very few particles. Composite Ferrogram densities were typically less than 1 percent.

4. Basically, four types of wear particles were observed: normal rubbing wear particles, spheres, nonferrous particles, and severe wear (spall) fragments. Fatigue microspall and laminar particles were not observed.

REFERENCES

1. Beerbower, A., "Spectrometry and Other Analysis Tools for Failure Prognosis," Lubr. Eng., 32, 6, pp 285-293 (1976).
2. Seifert, W. W., and Westcott, V. C., "A Method for the Study of Wear Particles in Lubricating Oil," Wear, 21, pp 27-42 1972.
3. Westcott, V. C., and Seifert, W. W., "Investigation of Iron Content of Lubricating Oil Using Ferrograph and an Emission Spectrometer," Wear, 23, pp 239-249 (1973).
4. Scott, D., Seifert, W. W., and Westcott, V. C., "Ferrography - An Advanced Design Aid for the 80's," Wear, 34, pp 251-260 (1975).
5. Reda, A. A., Bowen, R., and Westcott, V. C., "Characteristics of Particles Generated at the Interface Between Sliding Steel Surfaces," Wear, 34, 1975, pp 261-273 (1975).
6. Scott, D., Seifert, W. W., and Westcott, V. C., "The Particles of Wear. Sci. Am., 230, 5, pp 88-97 (1974).
7. Westcott, V. C., and Middleton, J. L., "The Investigation and Interpretation of the Nature of Wear Particles," Trans-Sonics, Inc., Burlington, Mass., Mar. 1974. (AD-A003553.)
8. Scott, D., and Mills, G. H., "Debris Examination in the SEM: A Prognostic Approach to Failure Prevention," Scanning Electron Microscopy Symposium, 7th, Chicago, 1974, Proceedings, Volume 1, IIT Research Institute, Chicago (1974), pp 883-888.
9. Scott, D., and Mills, G. H., "Spherical Debris - Its Occurrence, Formation and Significance in Rolling Contact Fatigue," Wear, 24, pp 235-242 (1973).

10. Bowen, E. R., and Westcott, V. C., Wear Particle Atlas, Naval Air Engineering Center, Lakehurst, N. J., July 1976.
11. Middleton, J. L., Westcott, V. C., and Wright, R. W., "The Number of Spherical Particles Emitted by Propagating Fatigue Cracks in Rolling Bearings," Wear, 30, pp 275-277 (1974).
12. Jones, W. R., Jr., and Parker, R. J., "Ferrographic Analysis of Wear Debris Generated in Accelerated Rolling-Element Fatigue Tests. ASLE Trans, 22, 1, pp 37-45 (1979).
13. Loewenthal, S. H., and Moyer, D. W., "Filtration Effects of Ball Bearing Life and Condition in a Contaminated Lubricant," ASME Paper 78-Lub-34, Oct. 1978.
14. Ruff, A. W., "Metallurgical Analysis of Wear Particles and Wearing Surfaces," NBSIR 74-474, National Bureau of Standards, 1974. (AD-778340.)
15. Christensen, C., "On the Origin of Spherical Particles Found on Fatigue Fracture Surface and Ferrograms," Wear, 53, pp 189-193 (1979).
16. Jones, W. R., Jr., "Spherical Artifacts on Ferrograms," Wear, 37, pp 193-195 (1976).

TABLE I. - PROPERTIES OF TETRAESTER LUBRICANT

Additives	Antiwear, oxidation inhibitor, antifoam
Kinematic viscosity, cS, at -	
311 K (100° F)	28.5
372 K (210° F)	5.22
477 K (400° F)	1.31
Flash point, K (°F)	533(500)
Fire point, K (°F)	Unknown
Autoignition temperature, K (°F)	694(800)
Pour point, K (°F)	214(-75)
Volatility (6.5 hr at 477 K (400° F)), wt. %	3.2
Specific heat at 477 K (400° F), J/(kg)(K)((Btu/lb)(°F))	2340(0.54)
Thermal conductivity at 477 K (400° F), J/(m)(sec)(K)((Btu/hr)(ft)(°F))	0.13(0.075)
Specific gravity at 477 K (400° F)	0.850

TABLE II. - SUMMARY OF BEARING FAILURES

Time of failure detection by accelerometer, hr	Weight loss, mg	Description of failure
443	118	One inner race spall 12.7 mm long; one ball with spall
526	62	One inner race spall 1 mm long by 2.5 mm wide; one outer race spall 6.4 mm long
1013	---	One inner race spall
1096	75	One outer race spall 5.6 mm long by 3.2 mm wide

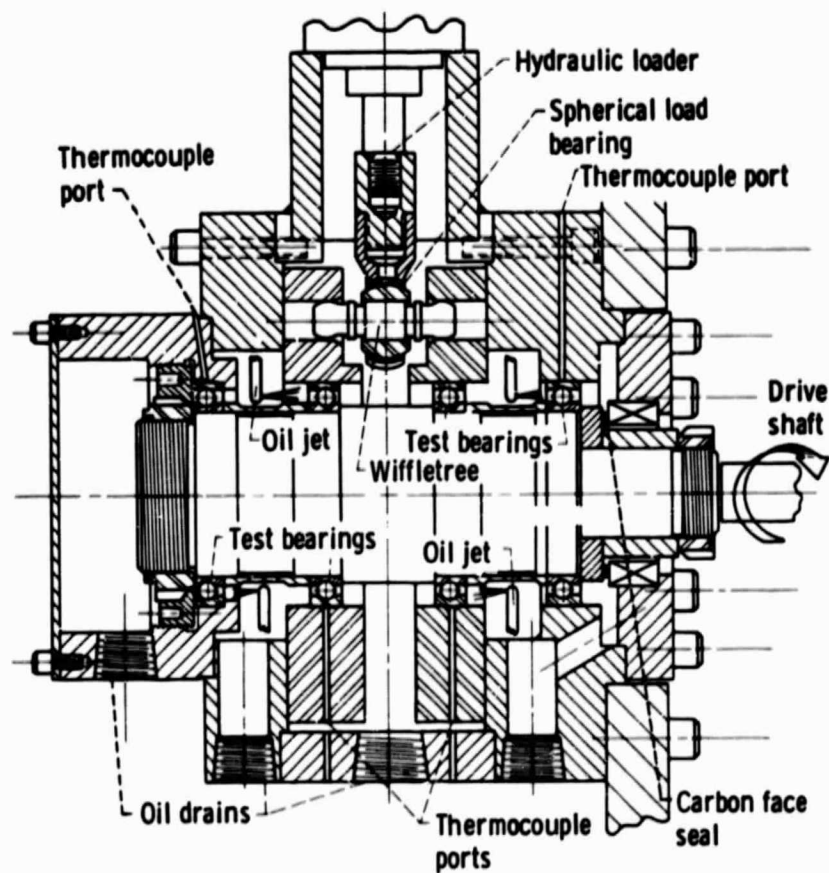


Figure 1. - Bearing fatigue tester.

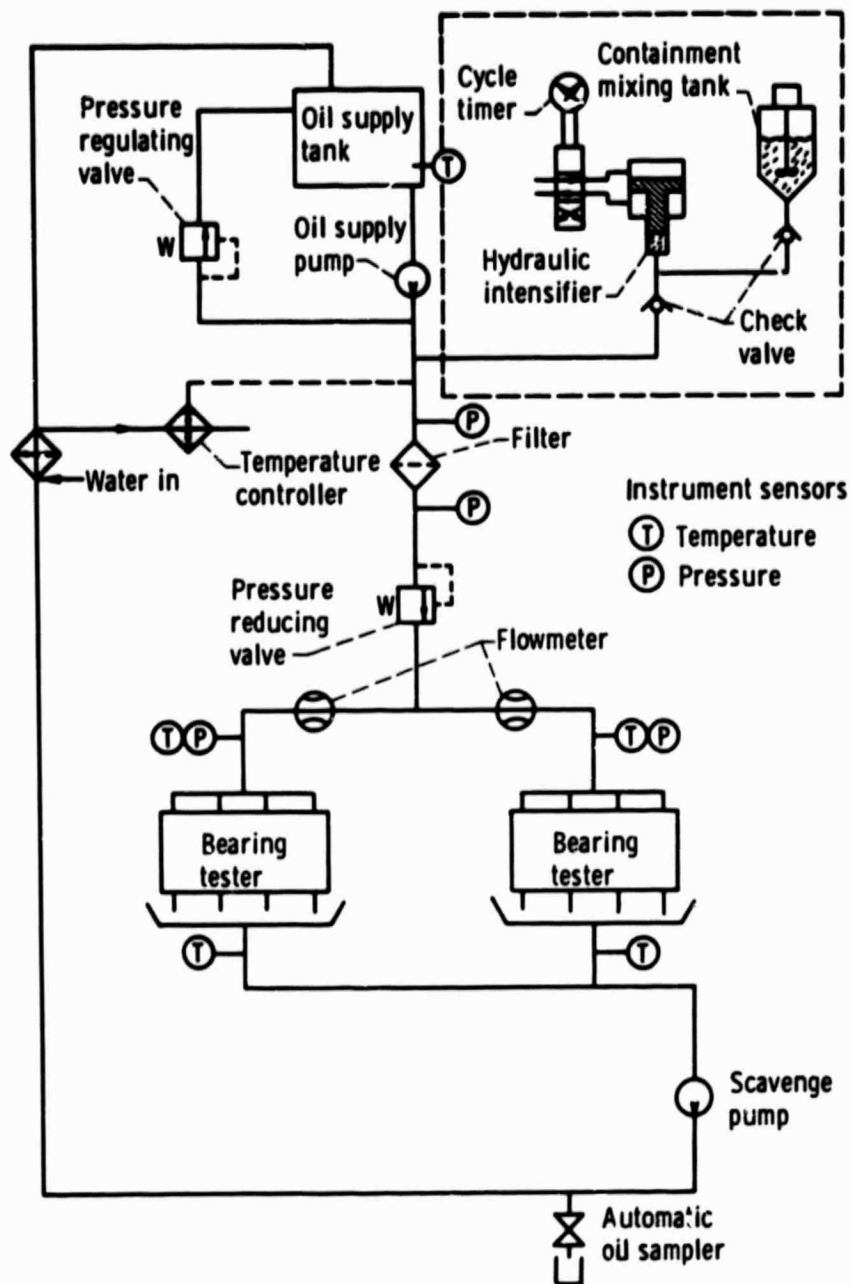


Figure 2. - Lubricant supply system.

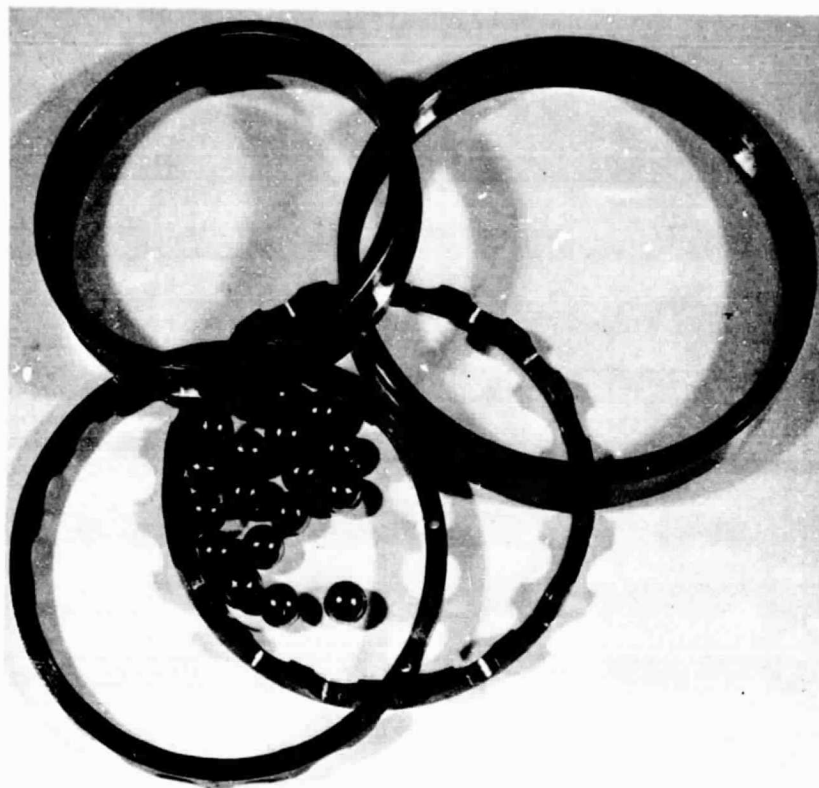


Figure 3. - Test bearing with 65-millimeter bore diameter.

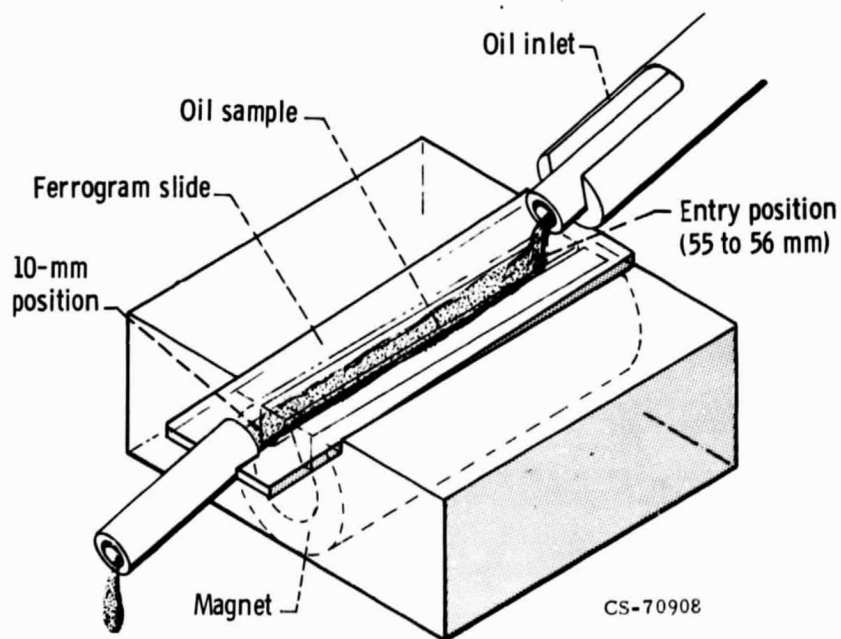
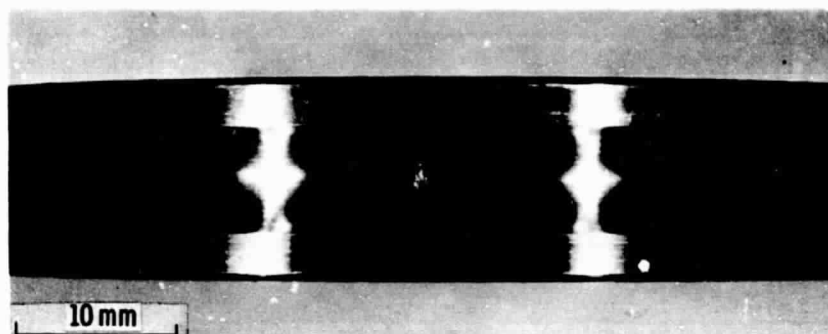
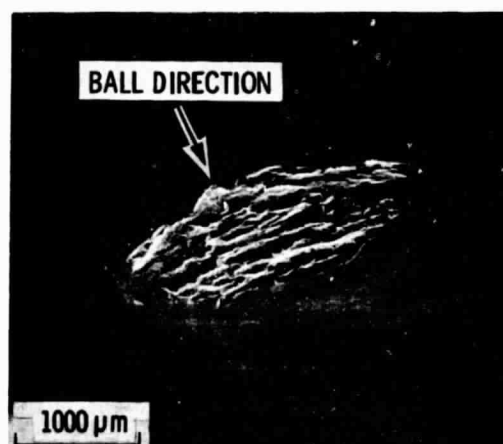


Figure 4. - Ferrograph analyzer.

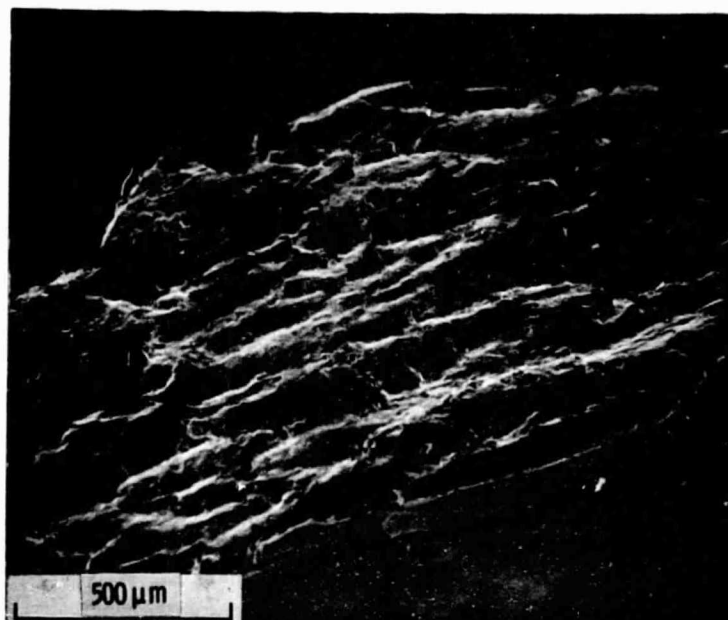


(a) FATIGUE FAILURE ON INNER RACE.



(b) FATIGUE SPALL UNDER LOW MAGNIFICATION.

Figure 5. - Apparent subsurface initiated fatigue spall on inner race of test bearing (526-hr failure).

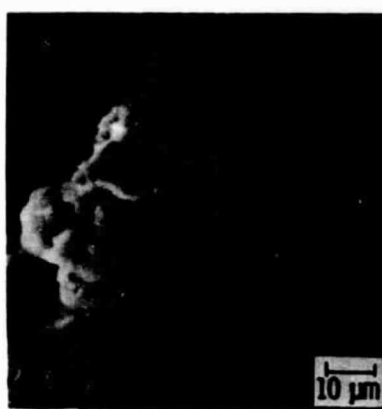


(c) LEADING EDGE OF SPALL UNDER MEDIUM MAGNIFICATION.

Figure 5. - Concluded.



(a) STRING OF WEAR PARTICLES AND 8 micrometer DIAMETER SPHERE FROM 530-hour SAMPLE.



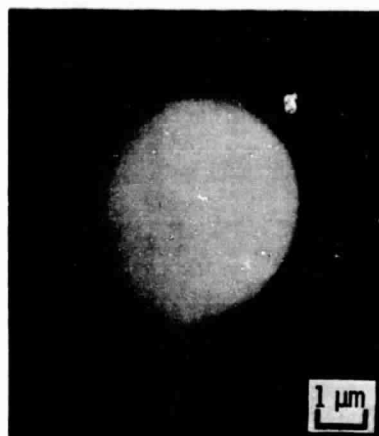
(b) AREA (a) AT HIGHER MAGNIFICATION.



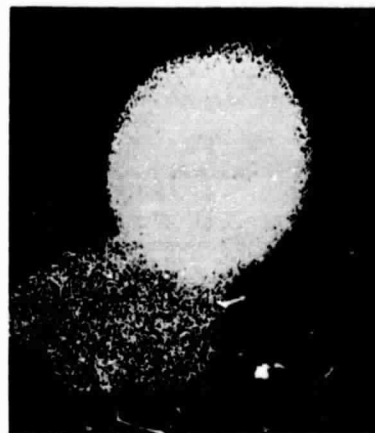
(c) X-RAY ENERGY MAPS OF (b) FOR IRON.

Figure 6. - Scanning electron micrographs.

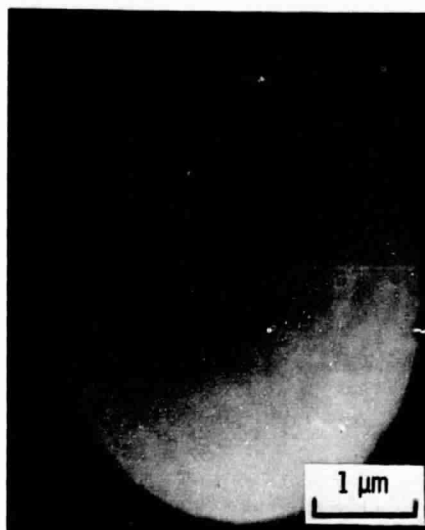
REPRODUCIBILITY OF THE
ORIGINAL PAGE IS POOR



(a)



(b)

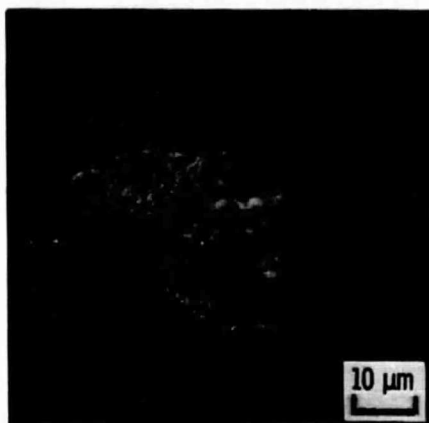


(c)

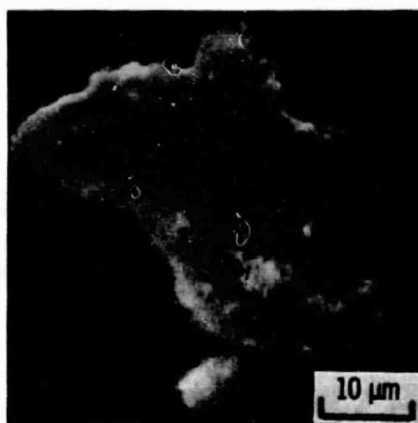


(d)

Figure 7. - Scanning electron micrographs of two spherical particles (a) and (c) and their corresponding iron X-ray energy maps (b) and (d). 530-Hour sample.



(a) BRONZE PARTICLE.



(b) SAME PARTICLE.



(c) OF (b) FOR COPPER.



(d) OF (b) FOR ZINC.

Figure 8. - Optical micrograph (a) and scanning electron micrograph (b) of same particle and their corresponding X-ray energy maps (c) and (d).

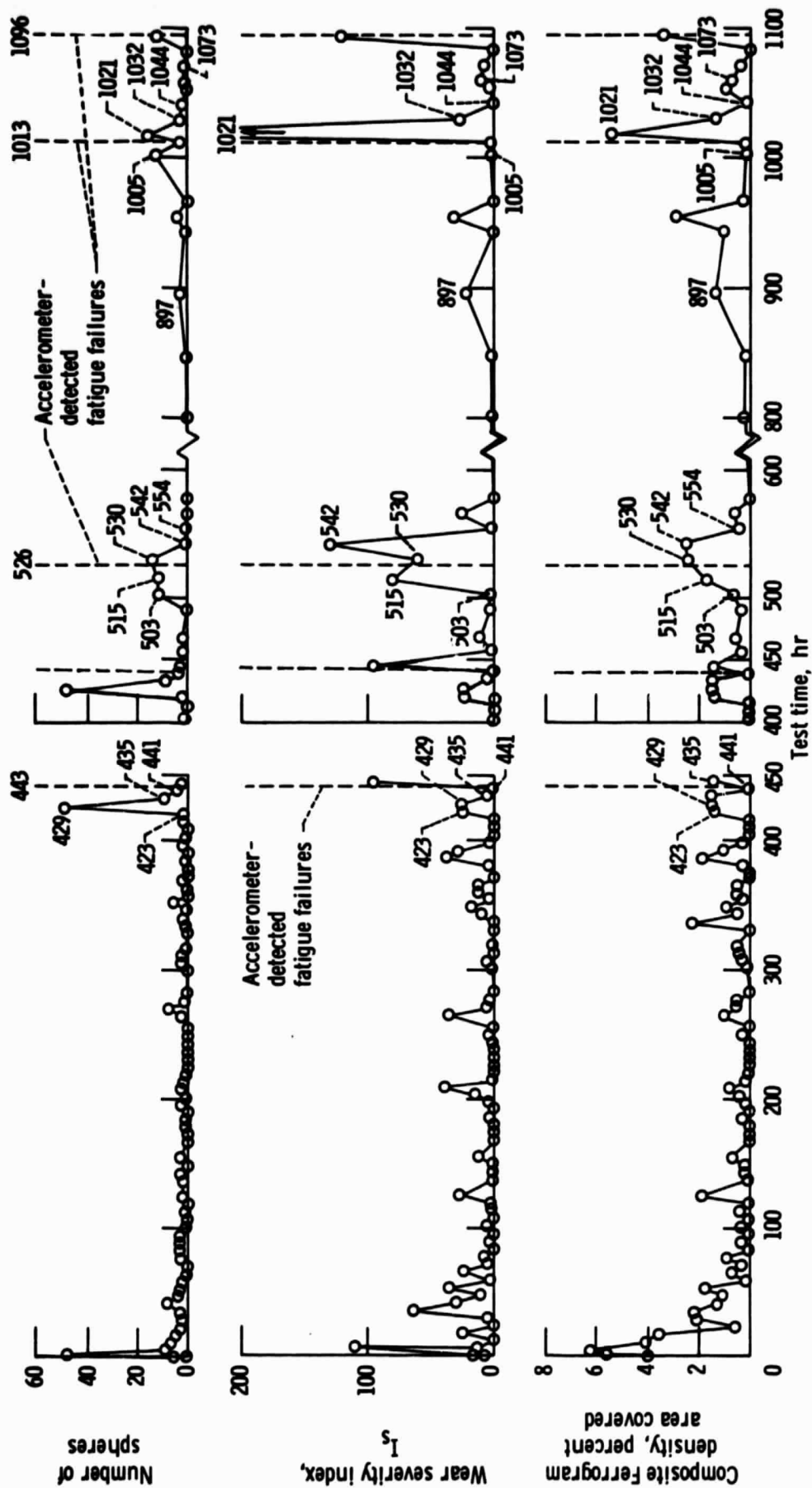


Figure 9. - Composite Ferrogram density, wear severity index, and number of spheres as functions of test time.

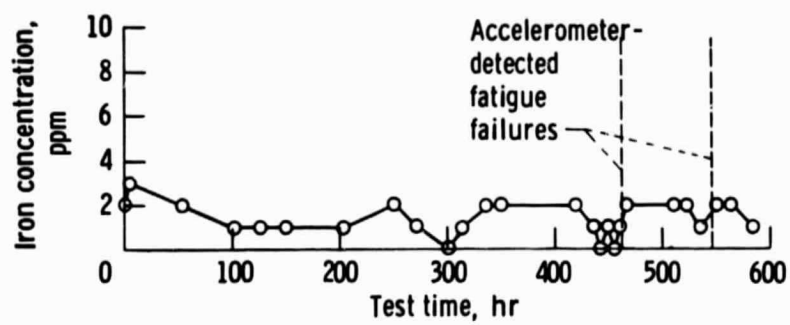


Figure 10. - Iron concentration in oil in ppm as function of time from spectrographic oil analysis (SOAP).

1. Report No. NASA TM-81403	2. Government Accession No.	3. Recipient's Catalog No.	
4. Title and Subtitle ANALYSIS OF WEAR DEBRIS FROM FULL-SCALE BEARING FATIGUE TESTS USING THE FERROGRAPH		5. Report Date	
		6. Performing Organization Code	
7. Author(s) William R. Jones, Jr. and Stuart H. Loewenthal		8. Performing Organization Report No. E-9827	
9. Performing Organization Name and Address National Aeronautics and Space Administration Lewis Research Center Cleveland, Ohio 44135		10. Work Unit No.	
		11. Contract or Grant No.	
12. Sponsoring Agency Name and Address National Aeronautics and Space Administration Washington, D.C. 20546		13. Type of Report and Period Covered Technical Memorandum	
		14. Sponsoring Agency Code	
15. Supplementary Notes			
16. Abstract <p>The Ferrograph was used to determine the types and quantities of wear particles generated during full-scale bearing fatigue tests. Deep-groove ball bearings made from AISI 52100 steel were used. A MIL-L-23699 tetraester lubricant was used in a recirculating lubrication system containing a 49-μm absolute filter. Test conditions included a maximum Hertz stress of 2.4 GPa, a shaft speed of 15 000 rpm, and a lubricant supply temperature of 74^o C (165^o F). Four fatigue failures were detected by accelerometers in this test set. In general, the Ferrograph was more sensitive (up to 23 hr) in detecting spall initiation than either accelerometers or the normal spectrographic oil analysis (SOAP). Four particle types were observed: normal rubbing wear particles, spheres, nonferrous particles, and severe wear (spall) fragments.</p>			
17. Key Words (Suggested by Author(s)) Ferrographic analysis; Spectrographic oil analysis; Rolling element fatigue; Wear mechanisms; Lubrication		18. Distribution Statement Unclassified - unlimited STAR Category 3⁷	
19. Security Classif. (of this report) Unclassified	20. Security Classif. (of this page) Unclassified	21. No. of Pages	22. Price*